

Article

# Investigation of Coated Cutting Tool Performance during Machining of Super Duplex Stainless Steels through 3D Wear Evaluations

Yassmin Seid Ahmed <sup>1,\*</sup> , Jose Mario Paiva <sup>1,2</sup> , Danielle Covelli <sup>3</sup> and Stephen Clarence Veldhuis <sup>1</sup> 

<sup>1</sup> McMaster Manufacturing Research Institute (MMRI), Department of Mechanical Engineering, McMaster University, 1280 Main Street West, Hamilton, ON L8S4L7, Canada; paivajj@mcmaster.ca (J.M.P.); veldhu@mcmaster.ca (S.C.V.)

<sup>2</sup> Department of Mechanical and Materials Science, Catholic University of Santa Catarina, Rua Visconde de Taunay, 427-Centro, Joinville-SC 89203-005, Brazil

<sup>3</sup> Biointerfaces Institute, McMaster University, ETB 422, 1280 Main Street West, Hamilton, ON L8S 0A3, Canada; dcovelli172@gmail.com

\* Correspondence: Seidahmy@mcmaster.ca; Tel.: +1-365-888-1186

Received: 17 July 2017; Accepted: 14 August 2017; Published: 17 August 2017

**Abstract:** In this study, the wear mechanisms and tribological performance of uncoated and coated carbide tools were investigated during the turning of super duplex stainless steel (SDSS)—Grade UNS S32750, known commercially as SAF 2507. The tool wear was evaluated throughout the cutting tests and the wear mechanisms were investigated using an Alicona Infinite Focus microscope and a scanning electron microscope (SEM) equipped with energy dispersive spectroscopy (EDS). Tribo-film formation on the worn rake surface of the tool was analyzed using X-ray Photoelectron Spectroscopy (XPS). In addition, tribological performance was evaluated by studying chip characteristics such as thickness, compression ratio, shear angle, and undersurface morphology. Finally, surface integrity of the machined surface was investigated using the Alicona microscope to measure surface roughness and SEM to reveal the surface distortions created during the cutting process, combined with cutting force analyses. The results obtained showed that the predominant wear mechanisms are adhesion and chipping for all tools investigated and that the AlTiN coating system exhibited better performance in all aspects when compared with CVD TiCN + Al<sub>2</sub>O<sub>3</sub> coated cutting insert and uncoated carbide insert; in particular, built-up edge formation was significantly reduced.

**Keywords:** super duplex stainless steel; tool wear mechanisms; tribo-films; chip characteristics; surface integrity

## 1. Introduction

Super duplex stainless steel (SDSS) is a specific type of stainless steel alloys that has a biphasic microstructure, consisting of approximately 50% ferrite and 50% austenite by volume. SDSS has a favorable combination of chromium, nickel and molybdenum [1], which provides an attractive combination of mechanical and corrosion properties and is thus widely applied in aggressive corrosion environments such as gas and oil, petrochemical and chemical, industries. These materials are considered difficult to machine because they have low thermal conductivity combined with high tensile strength and high shear strength and during machining they show a high tendency toward work-hardening [2–4]. These characteristics make SDSS more difficult to machine than standard austenitic stainless steels [5].

Adhesion (attrition), diffusion, abrasion and oxidation are the main wear mechanisms taking place during machining of stainless steels which are strongly associated with the temperature in the

cutting zone [6]. Another point found during machining of these alloys is the work hardening tendency. The work hardening of SDSS increases the friction forces during contact between the work piece and cutting tool edge, which increases the temperature, causing oxidation [7]. In addition, the high ductility of the stainless steel leads to the formation of long continuous chips and the intensive sticking of the workpiece material to the cutting tool surface, which results in an adhesive wear enhancement [8]. These conditions promote built-up edge (BUE) formation and tearing off during cutting, which results in cutting edge chipping and cutting forces instability. This response to the machining process results in severe surface damage to the machined part and chipping of the tool cutting edge [9]. Therefore, the selection of the cutting tool is very important to increase tool life, improve surface finish and reduce the cutting forces. Several papers have suggested the application of PVD coatings on the cutting tools as a way to reduce friction conditions during the cutting process by reducing heat generation [10]. For applications where the cutting process is characterized by high temperatures in the cutting zone, for instance, in machining of materials with low thermal conductivity, the use of cemented carbide tools coated with self-adaptive PVD coatings is strongly recommended. During machining, these coatings form protective, nano-scale tribo-films on the tool rake surface, which reduce friction and result in a reduction of the degree of BUE formation, leading to wear performance improvement [11].

Many researchers have studied the wear mechanisms associated with the machining of different types of stainless steels using CVD and PVD coated tools; however, there are few researchers who study in detail the wear mechanisms associated with machining SDSS. Corrêa et al. studied the machinability of two stainless steels, martensitic S41000 and super martensitic S41426, during turning with CVD TiC–TiCN–TiN coated tools. The authors found that abrasion and diffusion were the main wear mechanisms during machining of martensitic stainless steel, while for the super martensitic stainless steel, attrition and abrasion were dominant [6]. Krolczyk et al. [12] studied surface roughness and wear mechanisms through machining of duplex stainless steel (AISI S31803) with Ti(C/N)/Al<sub>2</sub>O<sub>3</sub>/TiN coated tools. The authors determined that the main wear mechanism was abrasion. Selvaraj et al. [13] also investigated machining of two types of duplex stainless steel and found that the wear mechanisms changed depending on the cutting speed. At low cutting speed, the main wear mechanism was abrasion, while diffusion and oxidation wear were predominant at high cutting speed. Carlos et al. [14] performed turning experiments with a super duplex stainless steel alloy (S32750) using a PVD multi-coated (TiAlN and TiN layers) cemented carbide tools. The authors noted that notch wear at the end of depth of cut was the responsible for the end of tool life and that a large amount of the material adhered to the tool wear area. Jawaid et al. [15] used CVD Ti(C/N)/TiC/Al<sub>2</sub>O<sub>3</sub> and PVD TiN coated inserts. The authors reported that attrition was the principal wear mechanism at lower speed conditions, while abrasion and diffusion wear mechanisms were the failure modes at higher speed conditions. They also found that CVD coated inserts exhibited the worst performance, owing to the greater effects of thermo-mechanical loads, coarse grain size, and higher Co-content (18% Co) of the carbide substrate. In contrast, the PVD coated insert gave better performance because of the thermal stability of the alumina coating.

The main goal of this paper is to compare the tool life, wear mechanisms and tribological performance of coated (PVD AlTiN, CVD TiCN + Al<sub>2</sub>O<sub>3</sub>) and uncoated cemented carbide inserts in the turning of super duplex stainless steel—Grade UNS S32750. The performance of these cutting tools will be evaluated in terms of tool life, chip formation, surface integrity and cutting forces. The novelty in this research is 3D wear evaluations of different coated and uncoated tools supported by Alicona Microscope, SEM, EDS and XPS analyses. This research will increase understanding of the main reasons for different wear mechanisms acting during turning of SDSS and thus to summarize some suggestions to increase tool life for industry, particularly in the oil and gas sector.

## 2. Experimental Procedures

### 2.1. Workpiece Material

In this work, cylindrical tubes of super duplex stainless steel—UNS S32750 were investigated during turning (roughing operations). The chemical composition and mechanical properties of the material are shown in Table 1. To reveal the workpiece microstructure, samples of the super duplex stainless steel were prepared, polished and etched with Beraha's solution (100 mL H<sub>2</sub>O + 20 mL hydrochloric acid (HCl) + 0.3–0.6 g of potassium metabisulfite). The microstructure of the SDSS workpiece generated during the cutting process was characterized using a Nikon ECLIPSE LV 100 microscope (Nikon Canada Inc., Mississauga, ON, Canada) equipped with UC30 camera. The microstructure and phase distribution of the material were analyzed using NIS Elements imaging software. Images of the microstructure of the workpiece were captured from five different areas and the percentage averages of austenite and ferrite phases were calculated using the NIS imaging software (version 4.0, Nikon Canada Inc., Mississauga, ON, Canada). This microstructure and average results are presented in Figure 1.

**Table 1.** Chemical composition and mechanical properties of S32750.

Elements	Chemical Composition (%)	Proof Strength (0.2% Yield) (Mpa)	Tensile Strength (Mpa)	Elongation	Hardness (HRC)
C	0.03				
Si	0.80				
Mn	1.2				
P	0.035				
S	0.02	550	800–1000	15	32
Cr	25				
Ni	7				
Mo	4				
N	0.24				

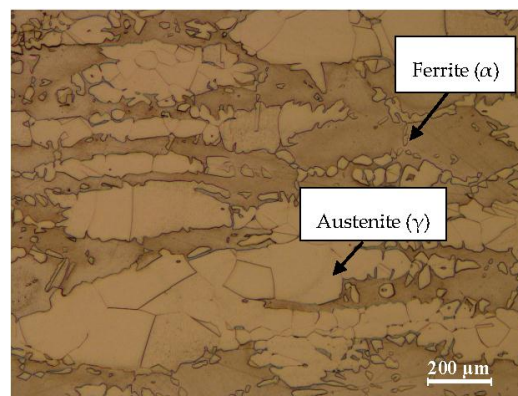


**Figure 1.** Microstructure of the SDSS UNS S32750 at 200× showing the distribution of each phase (Ferrite is continuous phase at 36% while Austenite is second phase at 64%).

### 2.2. Cutting Tools Characteristic and Cutting Fluid

Cemented carbide inserts coated with PVD AlTiN and CVD TiCN + Al<sub>2</sub>O<sub>3</sub> coatings were compared during cutting tests to determine the tool life. The cemented carbide is WC 6%Co and the ISO code for the cutting inserts is CNMG432-SM with the following geometry characteristics: Back rake angle,  $\lambda_0 = 9^\circ$ ; clearance angle,  $\alpha_0 = 5^\circ$ ; wedge angle,  $\beta = 76^\circ$ ; edge radius,  $r = 24 \mu\text{m}$  and nose radius,  $R_\epsilon = 0.8 \text{ mm}$ . The inserts were manufactured by Sandvik and the tool-holder

was an ISO PCLNL 45165 12HP, supplied by Kennametal. X-ray stress analysis was carried out on new coated tools according to the  $\sin^2 \Psi$  method to measure the residual stresses on the surface of the tools. The parameters used for residual stress analysis by X-ray diffraction were as follows: Bragg angle =  $118.2^\circ$ , Wave length = Co-Ka2, Passion ratio = 0.250,  $S1 = -7 \times 10^{-7}$  and  $\frac{1}{2} S2 = 3.5 \times 10^{-6}$ . The coating characteristics are shown in Table 2. The machining experiments were carried out on an OKUMA CNC Crown L1060 lathe (OKUMA, Charlotte, NC, USA) with 15 kW of power and an OKUMA OSP-U10L controller. The turning tests were conducted for roughing operations with a cutting speed of 120 m/min, feed rate of 0.3 mm/rev, and depth of cut of 1 mm, under wet conditions. The cutting fluid was applied at a flow rate of 11 L/min via a nozzle positioned directly above the cutting tool and directed toward the tool tip. The cutting fluid chosen was semi-synthetic coolant-CommCool™ 8800, manufactured by the Wallover Company (Harrow, ON, Canada), at a concentration of 7%, typically used with stainless steel alloys.

**Table 2.** Characteristics of coating systems.

Coating	Process	Layer	Structure	Residual Stresses (MPa)	Hardness (GPa)	Thickness ( $\mu\text{m}$ )	Roughness, $R_a$ ( $\mu\text{m}$ )
AlTiN	PVD	Monolayer	Columnar nano-crystalline [16]	$293 \pm 88$	35 [16]	1.8	0.039
TiCN + Al <sub>2</sub> O <sub>3</sub>	CVD	Bi layer	Columnar micro-crystalline [17]	$439 \pm 20$	31 [17]	Sublayer 5, Toplayer 3	0.038

### 2.3. Experimental Machine Techniques

During the machining tests, the cutting force measurements were performed with a 3D component tool holder Kistler dynamometer type 9121 with a data acquisition system. The signals of the forces from the dynamometer were transmitted to a Kistler 5010 type amplifier (Kistler Instrument Corp., Amherst, NY, USA) and then recorded on a computer using LABVIEW software (version 14.0, National Instruments, Austin, TX, USA). The acquisition rate was 300 data points per second, scale was 20 MU/volt and sensitivity was 3.85 mV/MU.

The tool flank wear was measured using a KEYENCE—VHX 5000 digital microscope (Keyence Corp., Osaka, Japan), equipped with a CCD camera and image analyzer software. The tool life criterion was set to a flank wear of 0.3 mm according to the recommendation of the ISO 3685 Standard [18]. After the tests, the cutting tools were analyzed by SEM (Vega 3-TESCAN, Brno, Czech Republic), coupled to EDS. The new and worn inserts were also analyzed using an Alicona Infinite Focus G5 microscope (Alicona Manufacturing Inc., Bartlett, IL, USA), which works by focus variation, to generate real 3D surface images. This microscope allows for the capture of images with a lateral resolution down to 400 nm and a vertical resolution down to 10 nm. In order to measure the total wear volume and BUE volume of a cutting edge, first a 3D model of a new edge of the original insert was measured and then the edge was measured a second time after cutting (0.3 mm flank wear). The software used the 3D image of the new edge as a reference and compared it with a 3D image of a worn edge. Following these measurements, all inserts were etched using hydrochloric acid (HCl) solution to remove all adhered material on the cutting tool to reveal the wear mechanisms.

The chip compression ratio, the shear angle and the friction coefficient at the tool-chip interface were determined according to standard procedures [19]. After the cutting test, the machined workpiece was investigated using SEM to reveal the surface distortion created during the cutting. In addition, the surface roughness of the machined workpiece was evaluated by means of an Alicona Infinite Focus-with the Profile roughness module. The procedures of surface roughness measurements were performed according to EN ISO standard 25178 [20]. Roughness measurements were taken with a cut-off wave length of 800  $\mu\text{m}$ , a vertical resolution of 100 nm and a lateral resolution of 2  $\mu\text{m}$ . The surface roughness used in this study is the arithmetic mean surface roughness value ( $R_a$ ), which is generally used in the industry. This evaluation was conducted three times and average reading was considered.

The structural and phase transformation at the cutting tool/workpiece interface, as well as the chemical nature of the tribo-films formed were determined by X-ray photoelectron spectroscopy (XPS) on a Physical Electronics (PHI) Quantera II (Physical Electronics Inc., Chanhassen, MN, USA). The XPS spectrometer was equipped with a hemispherical energy analyzer and an Al anode source for X-ray generation and a quartz crystal monochromator for focusing the generated X-rays. A monochromatic Al K $\alpha$  X-ray (1486.7 eV) source was operated at 50W–15 kV. The system base pressure was as low as  $1.33 \times 10^{-7}$  Pa with an operating pressure that did not exceed  $2.66 \times 10^{-6}$  Pa. Before any spectra were collected, the samples were sputter-cleaned for 4 min using a 4-kVAr<sup>+</sup> beam. A 200- $\mu$ m beam was used for all data collected on the samples. A pass energy of 280 eV was used to obtain all survey spectra, while a pass energy of 69 eV was used to collect all high resolution data. All spectra were obtained at a 45° take off angle. A dual beam charge compensation system was also utilized to ensure neutralization of all samples. The instrument was calibrated using a freshly cleaned Ag reference foil, where the Ag 3d<sup>5/2</sup> peak was set to 368 eV. All data analysis was performed using PHI Multipak version 9.4.0.7 software [7]. X-ray stress analysis was performed using X-ray diffraction on new coated tools to measure residual stresses on the surface of the tool, see Table 2.

### 3. Results and Discussion

#### 3.1. Tool Life Measurements

Figure 2 shows the plot of flank wear versus cutting length for the uncoated and coated cutting inserts tested during machining of SDSS. A significant improvement during machining in terms of tool life was obtained when machining with a cutting insert coated with PVD AlTiN. The results show that the PVD AlTiN coated cutting insert has a cutting length almost two times greater than the CVD TiCN + Al<sub>2</sub>O<sub>3</sub> coated cutting insert. The PVD AlTiN coating shows the ability to improve the friction conditions at the cutting interface, which leads to the rapid flow of the chip on the rake surface, as can be seen on the chip undersurface obtained with PVD AlTiN coating (Figure 3d). This behavior occurs due to the ability that AlTiN coating has to adapt to external stimuli, i.e., to self-organize. During the cutting process, a part of the cutting energy is consumed by self-organization of the coating layer to form a thermal barrier/lubricating tribo-film [21,22], which reduces the friction in the cutting zone and results in better tool life. The tool life obtained by CVD coated cutting inserts is shorter due to the intense friction conditions experienced in the cutting zone.

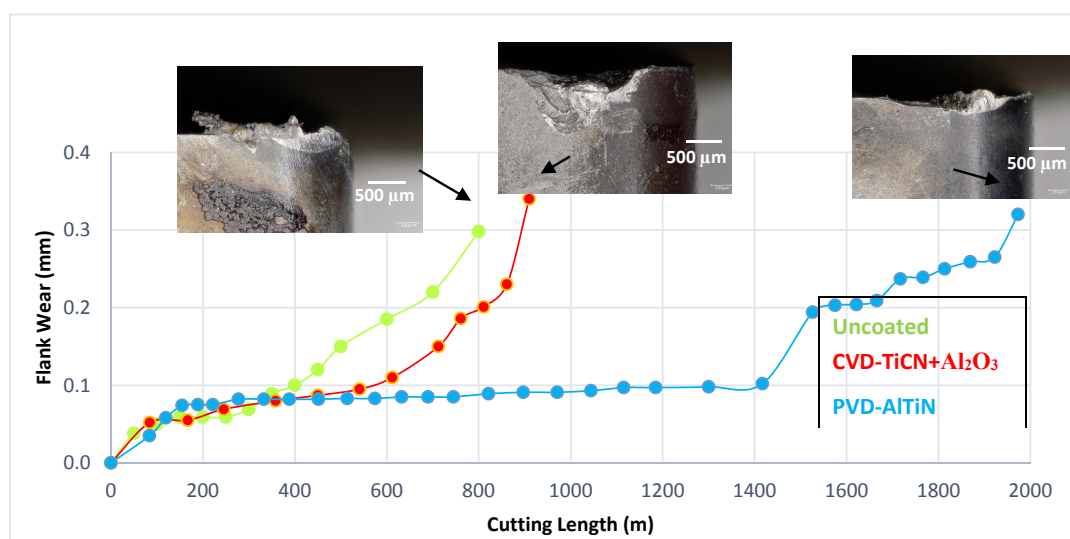


**Figure 2.** Relation between flank wear and cutting length for uncoated and coated carbide inserts during machining SDSS. Additionally the flank surface for each tool is presented at the end of tool life.

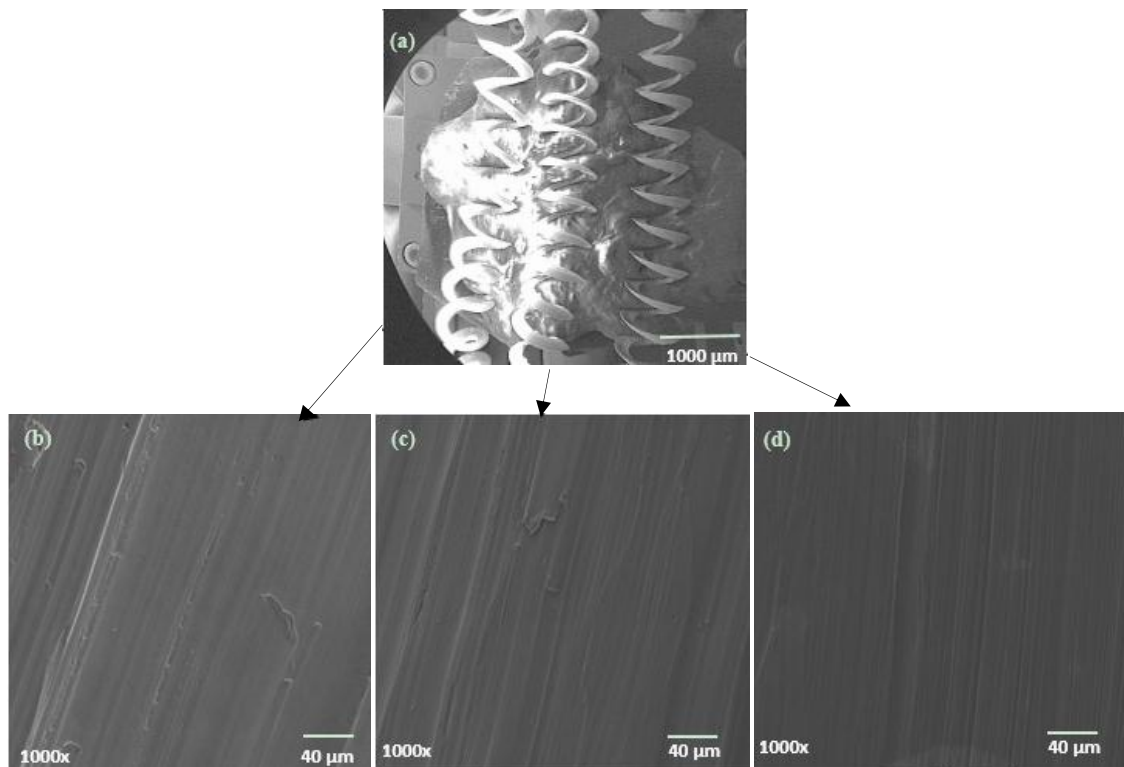


**Figure 3.** (a) General macrograph aspect of the chips, Chip undersurface obtained with (b) uncoated; (c) TiCN + Al<sub>2</sub>O<sub>3</sub>; and (d) AlTiN carbide inserts.

### 3.2. Chip Characteristics

Following machining, chip types and morphology were determined for each cutting tool. Figure 3 shows SEM images of the chips for the uncoated and coated tools; the chips have similar curling for both coatings. However, the chip undersurface morphology is better for the PVD AlTiN cutting insert. The high friction conditions at the chip-tool interface reduce the chip speeds during the chip flow, increasing the area of contact between tool and chip on the rake face surface and, therefore, contributing increased temperature in the cutting zone. High temperature due to high friction at the cutting zone results in reduced tool life for TiCN + Al<sub>2</sub>O<sub>3</sub> coated inserts.

Usually, the type of chip and undersurface morphology are direct indicators of frictional conditions at the tool-chip interface [19]. In this case, it is evident from chip characteristic studies that the friction conditions in the cutting zone (tool-chip interface) were more favourable for the AlTiN coating. The measured values of chip thickness and calculated values of the chip compression ratio, shear angle, and coefficient of friction are tabulated in Table 3. The chip thickness, chip compression ratio and shear angle are better for the AlTiN coated tool compared to CVD TiCN + Al<sub>2</sub>O<sub>3</sub> coated and uncoated tools (Table 3). These characteristics confirm the AlTiN coated tool has lower friction between the chip and tool, leading to lower wear of the cutting tool.

**Table 3.** Cutting characteristics during the turning operation of SDSS. Results were calculated according to standard procedures [19].

Type of Coating	Chip Thickness (mm)	Chip Compression Ratio	Shear Angle (°)	Coefficient of Friction	Tool Chip Contact Length (mm)
AlTiN	0.433	0.69	36	0.267	0.682
TiCN + Al <sub>2</sub> O <sub>3</sub>	0.560	0.54	29	0.404	0.797
Uncoated	0.653	0.46	27	0.445	0.903

A possible explanation of the observed improvement on the metal flow in the case of the AlTiN coated insert versus the CVD TiCN + Al<sub>2</sub>O<sub>3</sub> coated and uncoated tools is the formation of tribo-films on the rake surface during friction [23]. Smoother morphology of the chips (Figure 3d) during machining of SDSS using cutting tools with the AlTiN coated tool corresponds to better thermo-frictional conditions during cutting. In this case, a beneficial heat flow redistribution is taking place: The majority of the heat generated during cutting goes into the chips and dissipates with chip removal [24]. The tribo-films generated on the surface of PVD coated tool can change the wear behavior substantially: They provide surface protection, some lubricity and improve frictional and wear performance, resulting in very beneficial heat flow redistribution at the tool-chip interface. The presence of these tribofilms was confirmed by XPS investigation. This analysis was performed on the cutting tool (Rake face). Figure 4a shows the location selected for XPS studies.

### 3.3. The Composition of Tribo Films and Frictional Conditions

Figure 4b–d shows respectively the XPS Ti2p, Al2s and O1s spectra obtained from the rake surface of AlTiN coated cutting tool. The rake face was chosen for the analysis because of the elevated temperatures typically caused by tool-chip contact on this surface. The presence of Al<sub>2</sub>O<sub>3</sub> shows that a partial chemical transformation of aluminum, in the AlTiN coating, takes place during cutting (Figure 4c). The spectra also indicate the formation of an amorphous-like structure of the alumina-based tribo-films [25,26]. Titanium in the AlTiN coating (Figure 4b,d) forms non-stoichiometric titanium tribo-oxide and rutile TiO<sub>2</sub> (peaks 530.4, 457.4 and 463.8 eV). The formation of these tribo-films with high chemical stability reduces the adherence of the workpiece material to the cutting tool surface (Figure 5).

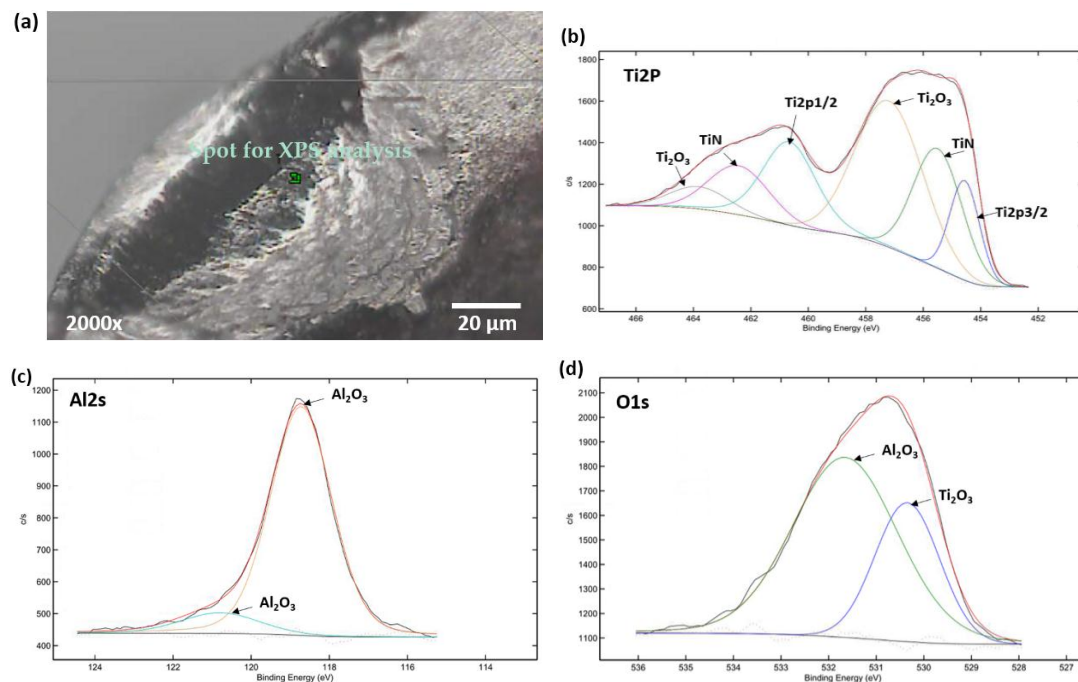


**Figure 4.** XPS data for tribo-films formed on the worn surface of AlTiN coating. (a) XPS spot on the AlTiN tool rake face; (b) AlTiN XPS high resolution spectra line for Ti2p; (c) AlTiN XPS high resolution spectra line for Al2s; and (d) AlTiN XPS high resolution spectra line for O1s.

In this way, the reduction of adhered material on the rake surface results in constant material flow, which leads to lower heat generation at the tool/workpiece interface. Due to the improved lubricity of this oxide under elevated cutting temperatures [27], the characteristics of the chips formed change critically (Figure 3) and the chip flow along the chip undersurface is also improved, which

improves the chip compression ratio (Table 3). These phenomena serve to enhance the adaptability of the coatings, which thus results in a better tool life (Figure 2). For this reason, formation of these nano-scale tribofilms is very beneficial on the surface of PVD coating in contrast to the microns thick alumina layer on the CVD coated tools.

To understand further why the PVD AlTiN coated tool has a better performance than CVD TiCN + Al<sub>2</sub>O<sub>3</sub> coated tool, the residual stresses of new PVD AlTiN and CVD TiCN + Al<sub>2</sub>O<sub>3</sub> coated tools were measured and listed in Table 2. It was found that the tensile residual stress in CVD TiCN + Al<sub>2</sub>O<sub>3</sub> is much higher (439 MPa) as compared to PVD AlTiN coated insert (293 MPa). The reason for that is the CVD coating process occurs under much higher temperature typically ranging from 200–1600 °C compared to lower than 500 °C in case of the PVD AlTiN coating [28]. High tensile residual stress in CVD coating induces internal stresses, which increase thermal loads and reduce thermal stability.

### 3.4. Tool Wear Analysis

As discussed previously, the main focus of this research is to compare different wear mechanisms of coated and uncoated inserts. For this reason, real 3D images of the worn tools were studied by means of an Alicona microscope, see Figure 5a. All the tools showed intense chipping, adhesion and flank wear during machining tests, which results in reduced tool life. The main reason for these behaviors is the instability in the chip formation temperature, combined with strong adhesion at the tool-chip interface resulting in high compressive stress; these phenomena are associated with low thermal conductivity of SDSS, which leads to high cutting temperature and accelerates the wear formation.

The presence of test material adhered onto the tools was observed in all tests. In order to analyze the wear mechanisms, it was necessary to remove the adhered layers of the cutting tools through chemical attack with HCl, see Figure 5b. It can be seen that there is no BUE on the surface of the tools, which means that all the adhered material was removed, allowing differentiation between wear mechanisms acting on the tools.

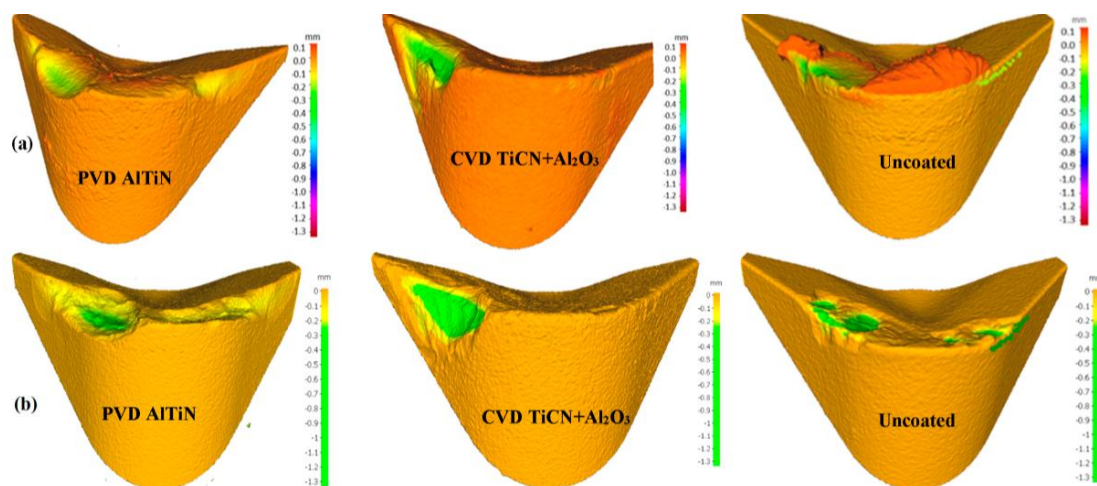


**Figure 5.** Alicona 3D images of the cutting tools after machining of SDSS (a) before, and (b) after etching showing the details of the cutting tools with their major wear mechanisms.

Each tool studied, total wear volume and the volume of BUE before and after etching were measured using the Alicona microscope. These results are presented in Figure 6. It is noted that the PVD AlTiN coated insert has the lowest total wear and BUE volume compared with the CVD TiCN + Al<sub>2</sub>O<sub>3</sub> coated and uncoated inserts, indicating that AlTiN coating exhibits good performance during machining of SDSS. This conclusion agrees with the results obtained from the XPS studies (Figure 4), where it is observed that the AlTiN coating has the capacity to adapt to external stimuli,

i.e., to self-organize. In this way, the tribo-film formation can enhance the process of cutting, which provides benefits such as reducing the friction conditions in the cutting zone, which leads to smoother chip undersurface (Figure 3d), reduction in BUE formation and increase in tool life (Figure 2) [11].

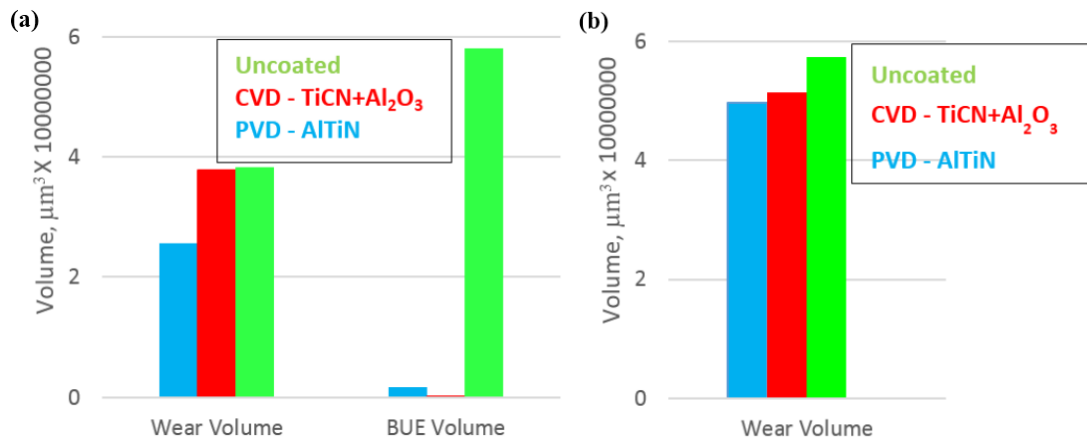


**Figure 6.** Comparison of total wear volume and BUE volume for uncoated and coated tools (a) before, and (b) after etching.

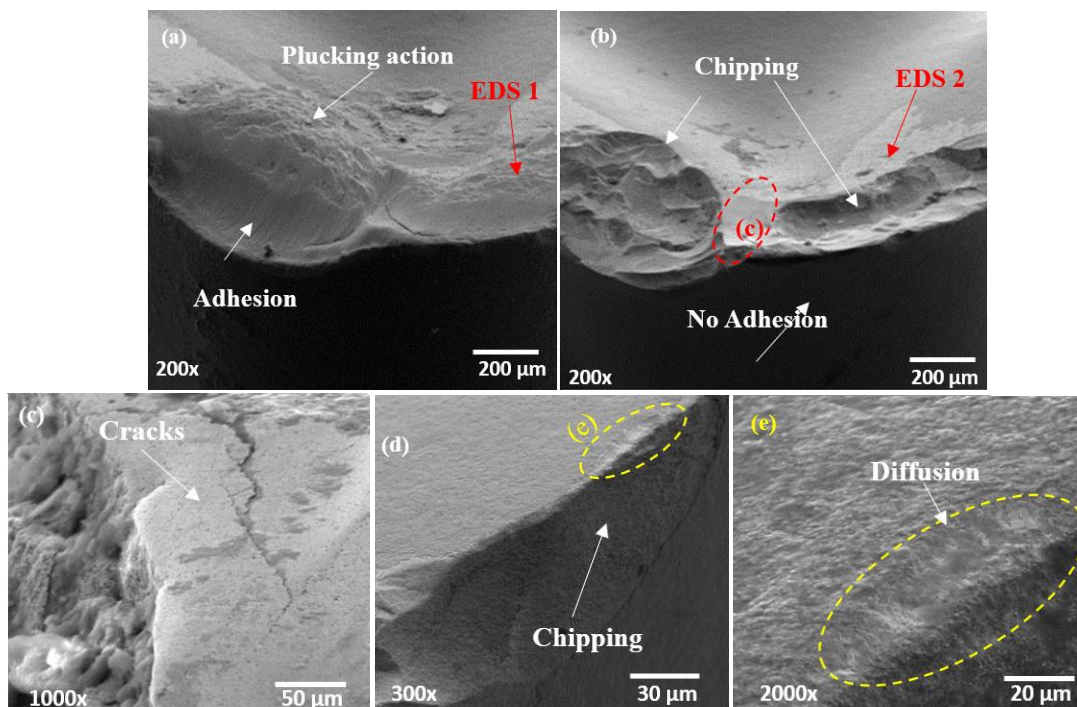
Different wear mechanisms commonly associated with machining of SDSS were observed during the wear tests, flank wear and chipping being the most significant modes. Also, material adhesion was observed in all cutting tools. As was explained in the previous paragraph, adhesive wear is the main wear mechanism during machining of stainless steels. However, after etching and at high magnifications, different wear mechanisms were observed. In the following paragraphs the different modes of wear are discussed, and associated EDS analysis are summarized in Table 4.

**Table 4.** EDS analysis associated with cutting tools in Figures 7–9.

EDS	Chemical Composition %								
	Fe	W	O	Cr	Ni	C	Ti	N	Al
1	26.3	7.55	30.37	16.04	4.25	23.49	0.54	–	1.41
2	0.11	2.10	20.2	1.20	0.30	14.00	2.54	12.50	49.20
3	34.06	1.37	13.12	15.9	3.92	24.95	3.00	–	0.75
4	0.11	0.92	54.45	–	0.10	28.7	0.56	–	29.13
5	0.11	66.4	13.00	1.13	–	23.00	0.1	–	0.50
6	44.2	0.8	15.00	18.0	8415	18.2	0.48	–	0.42

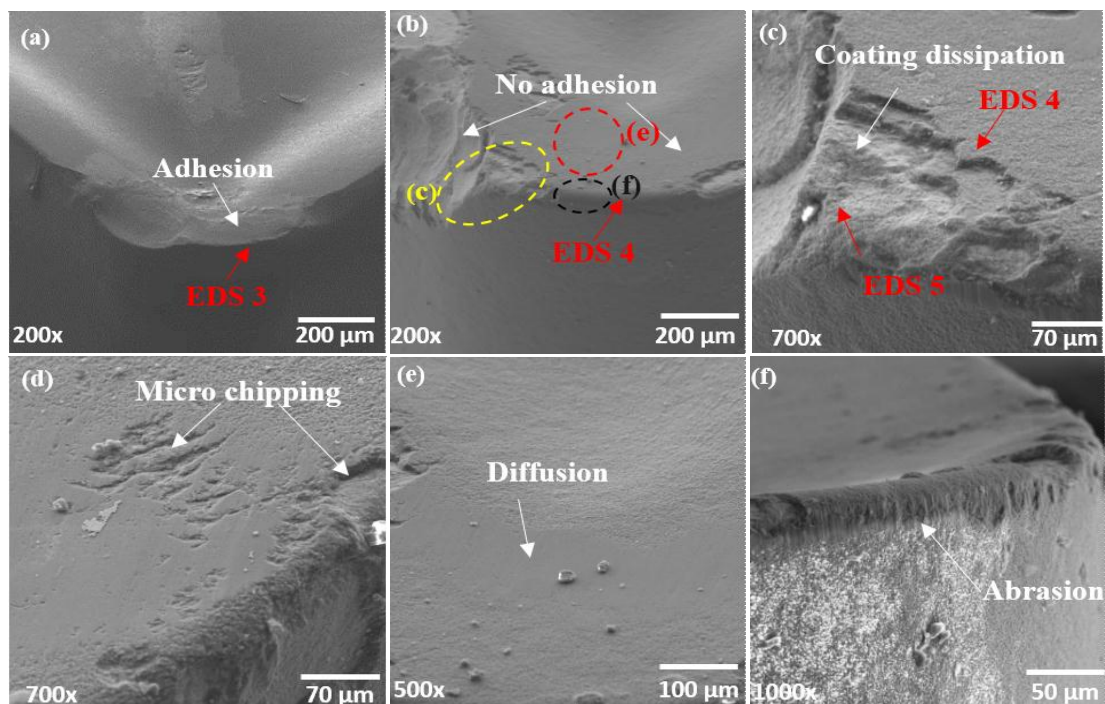
Figure 7 shows in detail the wear mechanisms of the PVD AlTiN coated insert. Figure 7a shows the tool before etching where the presence of adhered workpiece material was confirmed by EDS 1 (high percentage of Fe and Cr). Figure 7b–e show the same tool after etching, where there is no adhered material on the tool, see EDS 2. Figure 7a shows areas with a rough aspect on the cutting edge, which are characteristic of the adhesive (or attrition) wear mechanism [29]. This mechanism frequently occurs when there is chemical affinity between the tool and the workpiece material, and adhesion leads to the formation of BUE at the coated tool-chip interface. Another relevant phenomenon, which can be related to the tribological system behavior is the high tool-chip interface temperature: machining at a speed of 120 m/min generates high temperatures at the tool-chip interface that can generate adhesion on the tool rake and flank face as evidenced by plastic flow of the workpiece material (stick-slip, followed by plucking action). Similar results were reported by Corrêa et al. [6] and Junior et al. [30]. Figure 7c shows a high magnification of tool-adhered layer interface where a large crack is observed running perpendicular to the flank face. This crack could have been caused by one or a combination

of the following wear mechanisms [31]: Diffusion, adhesion, abrasion and oxidation. These wear mechanisms lead to a continual loss or dislocation of material. Also, BUE formation can lead to mass loss or mass dislocation as it grows throughout the cutting process and periodically breaks off, creating cracks on the tool surface and break-out the cutting edge [11]. Figure 7d shows intensive chipping developed on the cutting edge, which indicates that mechanical fatigue caused by BUE formation caused damage to the cutting tool [32]. Above the cutting edge in Figure 7e, there is a smooth surface, which is associated with diffusion wear. Diffusion wear is a mechanism that involves transport of the atoms from high concentration (cutting tool) to low concentration (chip) [19], which depends mainly on the cutting temperature, contact time and the solubility of the elements in the secondary shear zone [33]. This process takes place in a very narrow area at the interface between the cutting tool and chip and causes a weakening of the cutting tool.



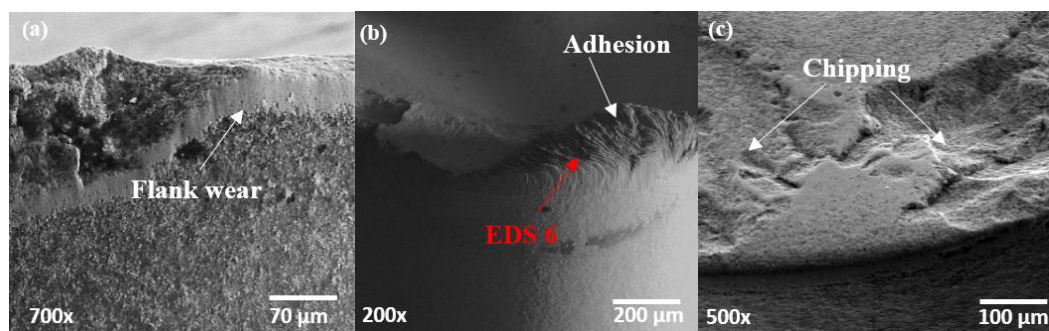
**Figure 7.** SEM images of PVD AlTiN coated insert after machining SDSS: (a) cutting tool before etching; (b) cutting tool after etching; (c–e) cutting tool with different magnifications.

Figure 8 shows the wear mechanisms of the CVD TiCN + Al<sub>2</sub>O<sub>3</sub> coated insert. Figure 8a shows the insert before etching and Figure 8b–f show the insert after etching, see EDS 3 and 4 in Table 4. Figure 8c shows the rake face of the tool where the coating was removed from the cutting tool. EDS 5 and 6 results identify two strips of the coating (EDS 4) on the substrate of the tool (EDS 5). The coating was exposed along the cutting edge, and severe chipping and micro-chipping developed (see Figure 8d). These mechanisms confirm the previous results obtained by X-ray stress analysis (Table 2). Due to high coating temperature, internal stress is induced, increases thermal loads and reduces thermal stability, leading to intensive chipping on the cutting edge. Figure 8e shows a very smooth surface, which is clearly seen at high magnification, suggesting that a diffusion wear mechanism prevailed on the rake face [31]. Figure 8f shows parallel lines in the direction of sliding action, which indicate abrasive wear. The ASTM International tool wear standard explains that abrasive wear occurs as a result of hard particles forced against and moved along a solid surface [34], which is in this case BUE fragments. Selvaraj et al. [13] explained that abrasion wear mechanism is caused by grains broken off during the turning process, which become restricted between the chip and the tool, creating scratches on the flank face of the tool. The same explanation was also suggested by Krolczyk et al. [11] and Jawaid et al. [15].



**Figure 8.** SEM images of CVD TiCN + Al<sub>2</sub>O<sub>3</sub> coated insert after machining SDSS: (a) cutting tool before etching; (b) cutting tool after etching; (c–f) cutting tool with different magnifications.

Figure 9 shows the different wear mechanisms on the surface of the uncoated insert before and after etching. Figure 9a shows the flank face of the tool after chemical etching, where a view of the regular flank wear is shown. Figure 9b shows the tool before etching where a large BUE is seen on the tool as indicated in EDS 6. After etching (Figure 9c), all the adhered material was removed revealing that severe chipping has occurred on the cutting edge.



**Figure 9.** SEM images of uncoated insert after machining SDSS. (a) Flank face after etching; (b) cutting tool before etching; and; (c) cutting tool with chipping.

In summary, after the turning of SDSS with different cutting tools, it is possible to see that, due to low machinability of SDSS, the tools are easily affected, leading to excessive tool wear during machining operations. To ensure good results with SDSS, it is necessary to understand how the cutting tool behaves during cutting. Under the cutting conditions tested, the cutting tools showed wear from various mechanisms: Adhesion, abrasion and diffusion. It is important for industry to understand the main reasons for these mechanisms in order to reduce their effect on tool life. A summary of the main causes of wear observed during cutting SDSS through this research and suggested solutions is given in Table 5.

**Table 5.** A summary of the main causes and suggested solutions of different wear mechanisms observed for uncoated and coated tools.

Cutting Tool	Wear Mechanism	Main Causes	Suggested Solutions
PVD AlTiN	Adhesive wear (Attrition)	High strain hardening High ductility	Use very low or very high cutting speeds to decrease the formation of BUE [19]
	Chipping	BUE formation	
	Diffusion	High cutting temperature	Increase the flow and pressure of the coolant to reduce the cutting temperature
CVD TiCN + Al <sub>2</sub> O <sub>3</sub>	Cracks	BUE formation	Use very low or very high cutting speeds to decrease the formation of BUE [19]
	Abrasive wear	BUE fragments	
	Adhesive wear (Attrition)	High strain hardening High ductility	
	Coating dissipation	High tensile residual stresses	Use PVD coated tools
	Chipping	Coating dissipation	
	Diffusion	High cutting temperature	Increase the flow and pressure of the coolant to reduce the cutting temperature
Uncoated	Adhesive wear (Attrition)	High strain hardening High ductility	Use very low or very high cutting speeds to decrease the formation of BUE [19]
	Chipping	Chip jamming	Use cutting tool with a proper chip breaker to be able to break chips [35]

### 3.5. Machined Workpiece Characteristics

Surface integrity plays an important role in many areas and has a great importance in the evaluation of machining accuracy. Many factors affect the surface conditions of machined parts, one of them being the cutting tool, which has a significant influence on the surface roughness. Stainless steel is a material generally used for applications requiring the greatest reliability, and therefore, any damage to the subsurface layers must be controlled [36].

For this reason, small pieces of the machined workpiece were cut off to be analyzed using the SEM to reveal the surface distortions created during the cutting process and Alicona microscope to measure the surface roughness. Figure 10 shows three-dimensional and SEM images of the machined workpiece along with cutting force data collected at the beginning of the turning process and the values of surface roughness measured after the cutting tests. In Figure 10a,b, the machined surfaces obtained with uncoated and CVD TiCN + Al<sub>2</sub>O<sub>3</sub> coated inserts show cracks and distortions. It can be seen that minor cracks were found and bad surface finish with low distortion was accomplished. As a result of intensive BUE formed on the uncoated insert (Figure 5a) and high friction generated during cutting, some of the chips welded onto the surface of the workpiece (227 µm). Zhou et al. [37] and Alabdullah et al. [38] observed the same phenomenon during machining of difficult-to-cut materials.

Chip sticking on the machined workpiece is consistent with the high cutting forces measured during cutting. In addition, there is a high variation of the values of cutting forces for the uncoated insert (Figure 10a), which indicates that high frictions conditions in the cutting zone were generated during the cutting process with the uncoated insert. This phenomenon is strongly diminished for the coated tools: The variations of cutting forces are smaller, surface roughness is lower and there is no chip sticking on the machined surfaces (Figure 10b,c), which is a significant improvement.

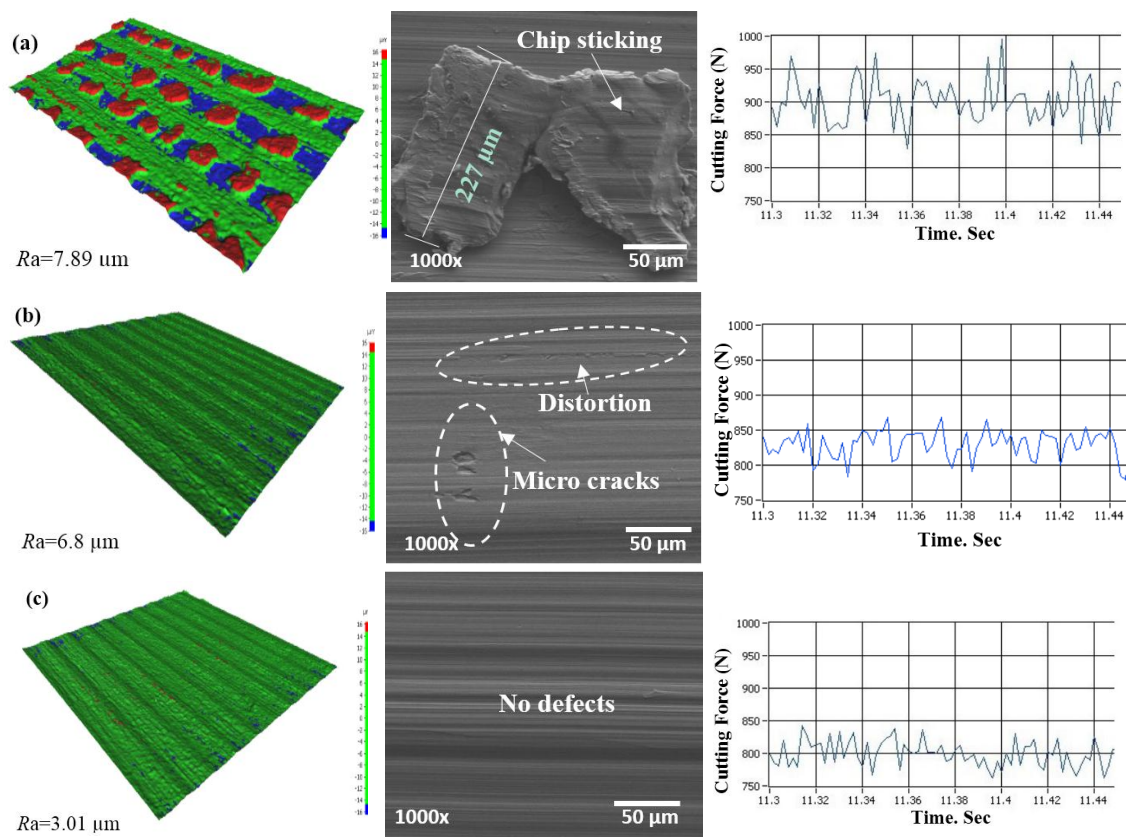


**Figure 10.** Three dimensional and SEM images of the machined surface obtained by (a) uncoated insert; (b) TiCN + Al<sub>2</sub>O<sub>3</sub>; (c) AlTiN insert and corresponding cutting forces and surface roughness values.

#### 4. Conclusions

The tool life results, analysis of wear mechanisms and tribological performance of different coated and uncoated tools during the turning of SDSS allowed the following conclusions to be drawn:

- Substantial improvement in tool life was achieved with the AlTiN coated insert: Tool life was approximately twice that of the CVD TiCN + Al<sub>2</sub>O<sub>3</sub> coated insert and three times than uncoated insert.
- The chip thickness, chip compression ratio and shear angle values are better for the AlTiN coated tool, compared to the CVD TiCN + Al<sub>2</sub>O<sub>3</sub> coated and uncoated tools, and the chip undersurface is smoother without any defects, indicating lower friction between the chip and tool rake face, which results in a constant chip flow over the tool rake surface.
- XPS analysis revealed that the underlying cause of the high performance of the AlTiN coating is the formation of aluminum oxide tribo-films at the tool-chip interface.
- The AlTiN coated tool had the lowest value for both BUE and total wear volume compared with the CVD TiCN + Al<sub>2</sub>O<sub>3</sub> coated and uncoated tools, indicating that PVD AlTiN coated tool performs very well with SDSS.
- Adhesion wear and chipping are the predominant wear mechanism for all the cutting tools studied. When turning with the PVD AlTiN coated tool, adhesion and diffusion were present in different places on the worn area of the tools. Machining with the CVD TiCN + Al<sub>2</sub>O<sub>3</sub> coated tool shows diffusion, abrasion, chipping and adhesion wear mechanisms while sever adhesion wear and chipping were the main wear mechanism with the uncoated insert.

- The machined surface obtained using the AlTiN coated tool had the lowest surface roughness value. The machined surfaces obtained with the CVD TiCN + Al<sub>2</sub>O<sub>3</sub> coated and uncoated inserts show minor cracks and distortions, and there is some chip sticking on the machined workpiece obtained by the uncoated insert, as a result of intensive BUE formation and high friction generated during cutting. Spikes in cutting forces at the beginning of the cutting process were highest for the uncoated cutting tool, which is directly related to chip sticking on the surface of the workpiece.

**Acknowledgments:** The authors would like to gratefully acknowledge the financial supported from the Natural Sciences and Engineering Research Council of Canada's (NSERC) Strategic Canadian Network for Research and Innovation in Machining Technology (CANRIMT).

**Author Contributions:** Yassmin Seid Ahmed performed the cutting experiments, performed metallographic, SEM, XRD and Alicona studies, and wrote the paper, Jose Mario Paiva planned experimental procedure, Danielle Covelli performed XPS studies, and Stephen Clarence Veldhuis is the supervisor of the research team. All authors have read and approved the final manuscript.

**Conflicts of Interest:** The authors declare no conflict of interest.

## References

1. Bordinassi, E.C.; Stipkovic, M.F.; Batalha, G.F.; Delijaicov, S.; Lima, N.B. Superficial integrity analysis in a super-duplex stainless steel after turning. *J. Achiev. Mater. Manuf. Eng.* **2006**, *18*, 335–338.
2. Biksa, A.; Yamamoto, K.; Dosbaeva, G.; Veldhuis, S.C.; Fox-rabinovich, G.S.; Elfizy, A.; Wagg, T.; Shuster, L.S. Wear behavior of adaptive nano-multilayered AlTiN/Me<sub>x</sub>N PVD coatings during machining of aerospace alloys. *Tribol. Int.* **2010**, *43*, 1491–1499. [[CrossRef](#)]
3. Paro, J.; Hänninen, H.; Kauppinen, V. Tool wear and machinability of HIPed P/M and conventional cast duplex stainless steels. *Wear* **2001**, *249*, 279–284. [[CrossRef](#)]
4. Nilsson, J.-O.; Kangas, P.; Wilson, A.; Karlsson, T. Mechanical properties, microstructural stability and kinetics of  $\sigma$  phase formation in 29Cr–6Ni–2Mo–0.38N in super duplex stainless steel. *Metall. Mater. Trans.* **2000**, *31*, 35–45. [[CrossRef](#)]
5. Nilsson, J.-O. Overview superduplex stainless steels. *Mater. Sci. Technol.* **1992**, *8*, 685–700. [[CrossRef](#)]
6. Corrêa, J.G.; Schroeterb, R.B.; Machadoa, A.R. Tool life and wear mechanism analysis of carbide tools used in the machining of martensitic and supermartensitic stainless steels. *Tribol. Int.* **2017**, *105*, 102–117. [[CrossRef](#)]
7. Paiva, J.M.; Torres, R.D.; Amorim, F.L.; Covelli, D.; Tauhiduzzaman, M.; Veldhuis, S.C.; Dosbaeva, G.; Fox-Rabinovich, G. Frictional and wear performance of hard coatings during machining of superduplex stainless steel. *Int. J. Adv. Manuf. Technol.* **2017**, *24*, 1–10. [[CrossRef](#)]
8. Endrino, J.L.; Fox-rabinovich, G.S.; Gey, C. Hard AlTiN-AlCrN PVD coatings for machining of austenitic stainless steel. *Surf. Coat. Technol.* **2006**, *200*, 6840–6845. [[CrossRef](#)]
9. Ciftci, I. Machining of austenitic stainless steels using CVD multi-layer coated cemented carbide tools. *Tribol. Int.* **2006**, *39*, 565–569. [[CrossRef](#)]
10. Sik, I.; Amanov, A.; Kim, J.D. The effects of AlCrN coating, surface modification and their combination on the tribological properties of high speed steel under dry conditions. *Tribol. Int.* **2015**, *81*, 61–72.
11. Fox-Rabinovich, G.S.; Paiva, J.M.; Gershman, I.; Aramesh, M.; Cavelli, D.; Yamamoto, K.; Dosbaeva, G.; Veldhuis, S.C. Control of self-organized criticality through adaptive behavior of nano-structured thin film coatings. *Entropy* **2016**, *18*, 290. [[CrossRef](#)]
12. Krolczyk, G.; Legutko, S.; Gajek, M. Predicting the surface roughness in the dry machining of duplex stainless steel DSS. *Metalurgija* **2013**, *52*, 259–262.
13. Selvaraj, P.D.; Chandramohan, P.; Mohanraj, M. Optimization of surface roughness, cutting force and tool wear of nitrogen alloyed duplex stainless steel in a dry turning process using Taguchi method. *Measurement* **2014**, *49*, 205–215. [[CrossRef](#)]
14. Carlos, O.J.; Anaelmo, E.D.; Rodnei, B. Correlating tool wear, surface roughness and corrosion resistance in the turning process of super duplex stainless steel. *J. Braz. Soc. Mech. Sci. Eng.* **2014**, *36*, 775–785.
15. Jawaid, A.; Olajire, K.; Ezugwu, O. Machining of martensitic stainless steels (JETHETE) with coated carbides. *Proc. Inst. Mech. Eng. Part B J. Eng. Manuf.* **2001**, *215*, 769–779. [[CrossRef](#)]
16. Aihua, L.; Jianxin, D.; Haibing, C.; Yang, C.; Jun, Z. Friction and wear properties of TiN, TiAlN, AlTiN and CrAlN PVD nitride coatings. *Int. J. Refract. Met. Hard Mater.* **2012**, *31*, 82–88. [[CrossRef](#)]

17. Dobrzański, L.A.; Pakuła, D.; Križ, A. Tribological properties of the PVD andCVD coatings put down onto the nitride tool ceramics. In Proceedings of the 12th International Scientific Conference: Achievements in Mechanical& Materials Engineering, Podgorica, Montenegro, 2–5 April 2003; pp. 267–270.
18. ISO 3685:1993–*Tool Life Testing with Single-Point Turning Tools*; International Organization for Standardization: Geneva, Switzerland, 1993.
19. Shaw, M. *Metal Cutting Principles*, 2nd ed.; Oxford University Press: New York, NY, USA, 2005.
20. ISO 25178–2–*Geometrical Product Specifications (GPS)—Surface Texture: Areal Part 2: Terms, Definitions and Surface Texture Parameters*; International Organization for Standardization: Geneva, Switzerland, 2012.
21. Fox-Rabinovich, G.; Totten, G.E. *Self-Organization during Friction: Advanced Surface-Engineered Materials and Systems Design*; CRC Press: Boca Raton, FL, USA, 2006.
22. Jacobson, S.; Hogmark, S. Tribofilms—On the crucial importance of tribologically induced surface modification. In *Recent Developments in Wear Prevention, Friction and Lubrication*; Nikas, G.K., Ed.; Research Signpost: Kerala, India, 2010.
23. Fox-Rabinovich, G.; Kovalev, A.; Veldhuis, S.; Yamamoto, K.; Endrino, J.L.; Gershman, I.S.; Rashkovskiy, A.; Aguirre, M.H.; Wainstein, D.L. Spatio-temporal behaviour of atomic-scale tribo-ceramic films in adaptive surface engineered nano-materials. *Sci. Rep.* **2015**, *5*, 8780. [[CrossRef](#)] [[PubMed](#)]
24. Kalss, W.; Reiter, A.; Derflinger, V.; Gey, C.; EndrinoInt, J.L. Study of PVD AlCrN coating for reducing carbide cutting tool deterioration in the machining of titanium alloys. *J. Refract. Metal. Hard Mater.* **2006**, *24*, 399. [[CrossRef](#)]
25. Bershadsky, L.I.B.I. Kostetsky and the general concept in tribology. *Trenie I Iznos (Russ. Frict. Wear)* **1993**, *14*, 6–18.
26. Takago, S.; Gotoh, M.; Sasaki, T.; Hirose, Y. The residual stress measurements of TiCN PVD films. *Adv. X-ray Anal.* **2002**, *45*, 365–370.
27. Ho, W.Y.; Huang, D.H.; Hsu, C.H.; Wang, D.Y. Corrosion behaviors of Cr(N,O)/CrN double-layered coatings by cathodic arc deposition. *Surf. Coat. Technol.* **2004**, *172*, 177–178. [[CrossRef](#)]
28. Joseph, R.D. *ASM Specialty Handbook: Tool Material-Technology and Engineering*; ASM International: Almere, The Netherlands, 1 January 1995; pp. 67–77.
29. Noordin, M.Y.; Venkatesh, V.C.; Sharif, S. Dry turning of tempered martensitic stainless tool steel using coated cermet and coated carbide tools. *J. Mater. Proc. Technol.* **2007**, *185*, 83–90. [[CrossRef](#)]
30. Junior, A.B.; Diniz, A.E.; Teixeira Filho, F. Tool wear and tool life in end milling of 15–5 PH stainless steel under different cooling and lubrication conditions. *Int. J. Adv. Manuf. Technol.* **2009**, *43*, 756–764. [[CrossRef](#)]
31. Trent, E.; Wright, P. *Metal Cutting*, 4th ed.; Butterworth–Heinemann: London, UK, 2000; p. 464.
32. Melo, A.C.; Milan, J.C.G.; Silva, M.B.; Machado, A.R. Some observations on wear and damage in cemented carbide tools. *J. Braz. Soc. Mech. Sci. Eng.* **2006**, *28*, 269–277. [[CrossRef](#)]
33. Diniz, A.E.; Marcondes, F.C.; Coppini, N.L. The performance evaluation of ceramic and carbide cutting tools in machining of stainless steels. In *Tecnologia da Usinagem dos Materiais*, 5th ed.; Artliber Editora: São Paulo, Brazil, 2006.
34. ASTM G40-15–*Standard Terminology Relating to Wear and Erosion*; ASTM: West Conshohocken, PA, USA, 1987; Volume 03.02, pp. 243–250.
35. Choi, J.P.; Lee, S.L. Efficient chip breaker design by predicting the chip breaking performance. *Int. J. Adv. Manuf. Technol.* **2001**, *17*, 489–497. [[CrossRef](#)]
36. Fahrion, M.E.; Brown, J.C.; Hassell, J.C. *Technical Basis For Improved Reliability Of 347H Stainless Steel Heavy Wall Piping in Hydrogen Service*; NACE International: San Diego, CA, USA, 2003.
37. Zhou, J.; Bushlya, V.; Avdovic, P.; Stahl, J.E. Study of surface quality in high speed turning of Inconel 718 with uncoated and coated CBN tools. *Int. J. Adv. Manuf. Technol.* **2012**, *58*, 141–151. [[CrossRef](#)]
38. Alabdullah, M.; Polishetty, A.; Littlefair, G. Microstructural and surface texture analysis due to machining in super austenitic stainless steel. *J. Metall.* **2016**, *2016*, 3685312. [[CrossRef](#)]

